RESEARCH PAPERS

Acta Cryst. (1999). B**55**, 259–265

Crystal lattice and phase transitions in $Na_4TiP_2O_9$ (NTP) and $Na_{4.5}FeP_2O_8(O,F)$ (NFP) superionic conductors as a function of high pressures and temperatures

B. Maximov,[a]* M. Sirota,[a] S. Werner[b] and H. Schulz[b]

[a]*Academy of Science of Russia, Institute of Crystallography, Leninsky pr. 59, 117333 Moscow, Russia, and* [b]*Universität München, Institut für Kristallographie und angewandte Mineralogie, Theresienstr. 41, D-80333 München, Germany. E-mail: maximov@rsa.crystal.msk.su*

(*Received 21 January 1998; accepted 25 August 1998*)

Abstract

The lattice dynamics of $Na_4TiP_2O_9$ (tetrasodium titanium diphosphorus nonaoxide, NTP) and $Na_{4.5}FeP_2O_8(O,F)$ (nonasodium diiron tetraphosphorus difluoride octadecaoxide, NFP) crystals, which are superionic conductors with Na^+-ion conductivity, were studied under high pressures. Lattice constants as a function of hydrostatic pressure were measured on a four-circle diffractometer using a high-pressure cell with diamond anvils. At 1.78 ± 0.15 GPa NTP undergoes a reversible phase transition from the modulated monoclinic (pseudo-orthorhombic) modification which is stable under atmospheric conditions. A similar phase transition in NTP is observed at 523 K. For NFP, it may be assumed that at least three phase transitions occur when the pressure increases from atmospheric to 12 GPa, at 1.39 ± 0.08, 4.52 ± 0.32, and 6.02 ± 0.02 GPa, as concluded from the change in the unit-cell parameters and in the color of the crystals: the color changes from ginger (dark orange) to pink at ~1.5–2.0 GPa pressure and to violet at ~6.0 GPa.

1. Introduction

$Na_4TiP_2O_9$ (NTP) and $Na_{4.5}FeP_2O_8(O,F)$ (NFP) crystals belong to a family of superionic conductors with Na^+-ion conductivity (Ivanov-Schitz & Sigaryev, 1990). Such crystals can be used for the production of solid-state batteries, which is why studies of their crystal structures under various external effects, in particular under high pressures, are relevant.

The crystal structures of these compounds have already been studied over a wide temperature range. In particular, four phase states were found for NTP between 293 and 800 K by X-ray diffraction techniques (Tamazyan *et al.*, 1994). We have studied these four phases at 743 K (Klokova *et al.*, 1993), 663 K (Bolotina *et al.*, 1993), 573 K (Maximov *et al.*, 1990), and 293 K (Maximov, Bolotina, Simonov *et al.*, 1994). Two of them, the monoclinic phase at 293 K and the orthorhombic phase at 663 K, are modulated crystal phases.

Only one phase transition, at $T \simeq 530$ K, was found in NFP within the same temperature range of 293–800 K. This phase transition is due to the formation of an incommensurately modulated phase and, as was shown by Maximov, Bolotina, Tamazyan & Schulz (1994), it should be thought of as similar to the phase transition which occurs in NTP at 633 K.

Detailed information is available about specific features of the structures, thermal phase transitions, and modulated states in these crystals (Tamazyan *et al.*, 1994; Klokova *et al.*, 1993; Bolotina *et al.*, 1993; Maximov *et al.*, 1990; Maximov, Bolotina, Simonov *et al.*, 1994; Maximov, Bolotina, Tamazyan & Schulz, 1994), and could therefore be used as the basis for studying the influence of high pressures on the structural characteristics of NTP and NFP, which is the aim of this paper.

2. Sample preparation

Both compounds were grown from a melt by Dr V. A. Timofeeva (Institute of Crystallography, RAS). Oxyfluoride mixtures were used for the preparation of the NFP crystals, which is why F^- ions are present in the samples. When pure oxide mixtures were used, all attempts to obtain NFP crystals were unsuccessful. There are no F^- ions in the NTP crystals; these were the product of a solid-state reaction in which Na_2CO_3, TiO_2 and $NH_4H_2PO_4$ were used as the starting reagents.

3. Specific features of the crystal structures

Table 1 comprises a scheme of thermal phase transitions in NTP and NFP which permits the analysis of successive changes in the matrix of the crystal lattice and space-group symmetry in these compounds.

$\{M_2[PO_4]_4X_2\}_\infty$ radicals (M = Ti, Fe; X = O, F), which are endless in the [001] direction, are the main building blocks of the crystal structures of both compounds. These radicals are chains of corner-sharing M octahedra, $[MX_5]_\infty$, and are zigzag-shaped owing to

the alternate pulling together of apices of neighboring octahedra by pairs of $[PO_4]$ tetrahedra (Fig. 1*a*). The radicals are linked *via* Na polyhedra, shown in Fig. 1(*b*) by dashed lines. Crystallographic sites inside the polyhedra thus marked are fully occupied by Na atoms. The remaining Na atoms in the superionic phases of these compounds partially occupy their sites and ensure ionic transport in these crystals.

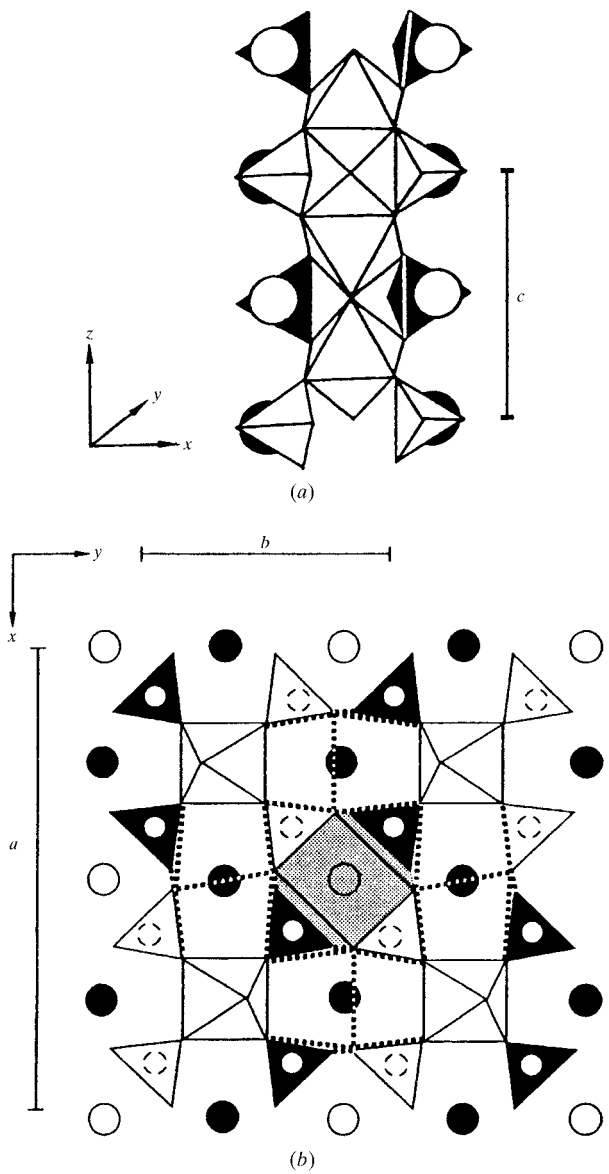

Fig. 1. The crystal structure of NTP crystals at 743 K. (*a*) The $\{Ti[PO_4]_4O_2\}$ infinite chain in the [001] direction. The unshaded octahedra represent TiO_6 octahedra and the tetrahedra represent PO_4 tetrahedra. Circles represent Na atoms located between translationally equivalent PO_4 tetrahedra. (*b*) The NTP crystal structure projected on the *xy* plane. One can see the mutual arrangement of the main building blocks of composition $\{Ti_2[PO_4]_4O_2\}$ in the paraphase at 743 K. The filled circles denote fully occupied Na positions and open circles indicate partly filled positions.

Table 1. *Structural phase transitions in NTP and NFP crystals*

$Na_4TiP_2O_9$ (NTP)	$Na_{4.5}FeP_2O_8(O,F)$ (NFP)
Phase (I), T = 743 K	
Space group *Bmcm*	
a = 15.752 (1) Å	
b = 7.524 (1) Å	
c = 7.094 (1) Å	
Phase transition at ~723 K (reversible)	
Phase (II), T = 663 K	Phase (I), T = 623 K
Bmcm (0,1/2,1−γ)s00, γ = 0.2	*Bmcm* (0,1/2,1−γ)s00, γ = 0.267
a = 15.711 (3) Å	a = 15.645 (1) Å
b = 7.516 (1) Å	b = 7.433 (1) Å
c = 7.090 (1) Å	c = 7.144 (1) Å
$\mathbf{q}$ = 1/2$\mathbf{b}^*$ + (1−γ)$\mathbf{c}^*$	$\mathbf{q}$ = 1/2$\mathbf{b}^*$ + (1−γ)$\mathbf{c}^*$
Phase transition at ~633 K (reversible)	Phase transition at 530 K (reversible)
Phase (III), T = 573 K	Phase (II), T = 293 K
Bmcm (0,β,1)s00, β = 0.5	*Bmcm* (0,β,1)s00, β = 0.5
a = 15.647 (8) Å	a = 15.520 (1) Å
b = 7.445 (4) Å	b = 7.410 (1) Å
c = 7.090 (5) Å	c = 7.119 (1) Å
$\mathbf{q}$ = $\mathbf{c}^*$+1/2$\mathbf{b}^*$	$\mathbf{q}$ = $\mathbf{c}^*$+1/2$\mathbf{b}^*$
Phase transition at ~523 K (reversible)	
Phase (IV), T = 293 K	
*B*2/*c* (3γ,0,γ)0s_2, γ = 0.2	
a = 15.492 (2) Å	
b = 7.545 (1) Å	
c = 7.047 (1) Å	
β = 92.06 (2)°	
$\mathbf{q}$ = 3$\gamma\mathbf{a}^*$+$\gamma\mathbf{c}^*$	

A relatively weak connection between the $\{M_2[PO_4]_4O_2\}$ radicals determines the flexibility of the framework of the crystal structures, which manifests itself in the experimentally found sequence of thermal phase transitions in NTP and NFP, and in the occurrence of modulated states.

As one can see from Table 1, the phase of NTP studied by us at 743 K has the highest symmetry of all the phases under study. This phase does not possess any other features of pseudosymmetry and it can be regarded as the basis for all lower-temperature NTP and NFP modifications. As a result of phase transitions upon lowering the temperature, the basic structure becomes distorted and some atoms are displaced from their average sites. As we showed earlier (Maximov, Bolotina, Tamazyan & Schulz, 1994), the character of the atomic displacement with regard to the average sites of the basic structure can be described by corresponding modulation parameters. The positions of the superstructure (satellite) reflections which occur in such phase transitions are defined by the corresponding wave vectors $\mathbf{q}$.

Table 2. *Unit-cell parameters of NTP as a function of increasing and decreasing pressure*

Rules indicate phase transitions.

p (GPa)	a (Å)	b (Å)	c (Å)	β (°)	V (Å^3)
Atmospheric	15.492 (2)	7.545 (1)	7.047 (1)	92.06 (2)	823.1 (2)
0.85 (5)	15.433 (2)	7.504 (2)	7.018 (1)	92.04 (2)	812.2 (2)
1.02 (5)	15.421 (2)	7.490 (1)	7.016 (1)	92.06 (2)	809.7 (2)
1.50 (5)	15.414 (2)	7.488 (1)	7.009 (1)	92.08 (2)	808.3 (2)
1.63 (5)	15.399 (2)	7.487 (1)	7.006 (1)	92.06 (2)	807.1 (2)
1.80 (5)	15.103 (2)	7.512 (2)	7.020 (6)	90.33 (6)	796.4 (5)
1.92 (5)	15.532 (3)	7.180 (2)	7.044 (2)	90.01 (3)	785.6 (4)
2.24 (5)	15.524 (3)	7.174 (1)	7.039 (3)	90.02 (2)	783.9 (3)
2.40 (5	15.507 (4)	7.163 (2)	7.033 (3)	90.01 (2)	781.2 (4)
3.00 (5)	15.492 (5)	7.156 (2)	7.015 (4)	90.02 (2)	777.7 (5)
3.00 (5)	15.492 (5)	7.156 (2)	7.015 (4)	90.02 (2)	777.7 (5)
2.40 (5)	15.507 (2)	7.163 (2)	7.033 (1)	90.01 (2)	781.2 (2)
2.01 (5)	15.536 (2)	7.180 (2)	7.045 (2)	90.02 (2)	785.9 (2)
1.83 (5)	15.537 (3)	7.173 (2)	7.041 (1)	90.02 (2)	784.7 (2)
1.60 (5)	15.538 (2)	7.173 (1)	7.042 (1)	90.03 (2)	784.8 (1)
1.42 (5)	15.535 (2)	7.170 (1)	7.040 (1)	90.05 (5)	784.3 (1)
1.23 (5)	15.539 (2)	7.174 (1)	7.042 (1)	90.04 (3)	785.0 (1)
0.92 (5)	15.547 (2)	7.177 (1)	7.045 (2)	90.03 (3)	786.1 (1)
0.68 (5)	15.022 (2)	7.601 (1)	7.029 (1)	90.51 (3)	802.6 (1)
0.50 (5)	15.472 (3)	7.541 (2)	7.038 (2)	90.96 (4)	820.9 (2)
0.34 (5)	15.485 (3)	7.544 (1)	7.042 (2)	92.16 (3)	822.7 (2)
Atmospheric	15.494 (3)	7.545 (1)	7.048 (1)	92.10 (4)	823.9 (2)

4. X-ray measurements under high pressures

X-ray measurements in a high-pressure cell with diamond anvils were made on a CAD-4 four-circle diffractometer with graphite monochromated Mo $K\alpha$ radiation. In our investigation we used a modified Merrill–Bassett-type cell (Merill & Bassett, 1974). Inconel 718 steel plates ~250 μm thick measuring 10×10 mm were used as a gasket between the diamonds. A methanol–ethanol mixture (4:1) was used as the hydrostatic liquid. This limited the maximum pressure to 12 GPa. Pressures in the cell were measured by the ruby fluorescence technique. 25 reflections within the Bragg-angle range 25–30° were used to refine the lattice parameters. Reflection intensities were measured over a hemisphere of the reciprocal lattice using the ω-scan technique.

Plate-like samples were used for X-ray diffraction measurements. The sample thickness did not exceed 100 μm and transversal sizes did not exceed 250 μm. The crystallographic [100] direction was perpendicular to the plane of the plates in all the samples we used. Altogether two NTP and six NFP single crystals were investigated. For the NTP crystals, lattice parameters as a function of pressure were measured under pressures ranging from atmospheric to 3 GPa. A small array of integrated intensities which we used to detect any changes of space-group symmetry in the NTP crystals was obtained at 2.24 (5) GPa. For the NFP crystals, the lattice dynamics were studied under pressures ranging from atmospheric to 12 GPa. Again, small arrays of integrated intensities were obtained at 4.00 (5) and 10.00 (5) GPa. It should be noted that the NTP crystals under study were fully destroyed under pressures in the range 2.5–3.0 GPa and they did not withstand cycling of the phase transition observed by us at 1.8 GPa. In contrast, NFP crystals were stable within the entire pressure range investigated and they did withstand cycling of the three phase transitions.

5. High-pressure results

5.1. *NTP crystals*

Refined parameters of an NTP basis lattice, which is pseudo-orthorhombic at atmospheric pressure and room temperature within pressures ranging from atmospheric to 3.0 GPa, are listed in Table 2. Figs. 2(*a*)–2(*e*) show them plotted as a function of pressure.

The changes in the lattice parameters reveal that under pressures of 1.78 ± 0.15 GPa a first-order phase transition occurs in NTP crystals. In fact, within a pressure range of 0.15 ± 0.05 GPa, the values of all the parameters (V, a, b, c, β) of the basis lattice change abruptly, while the crystal symmetry changes from monoclinic to orthorhombic. The jump in the volume is 2.4%. At 1.80 (5) GPa, within the pressure range of the transition, the monoclinic angle β is 90.33 (6)°.

The unit-cell parameter *a* decreases within the pressure range of the phase transformation, but in the high-pressure phase *a* is longer than at normal conditions. The opposite is true for the unit-cell parameter *b*, which is elongated during the transformation and shorter in the high-pressure phase. Owing to the rigid chains of $\{Ti_2[PO_4]_4O_2\}_\infty$ radicals oriented along [001], the changes in the unit-cell parameter *c* are comparatively small. The *c* parameter of the high-pressure phase is also elongated with respect to the phase stable at normal conditions. At pressures within the pressure range of the transformation, the value of *c* is intermediate between the two adjacent phases.

We have shown before that at atmospheric pressure and room temperature NTP crystals are monoclinic, microtwinned, and have a superstructure (Maximov,

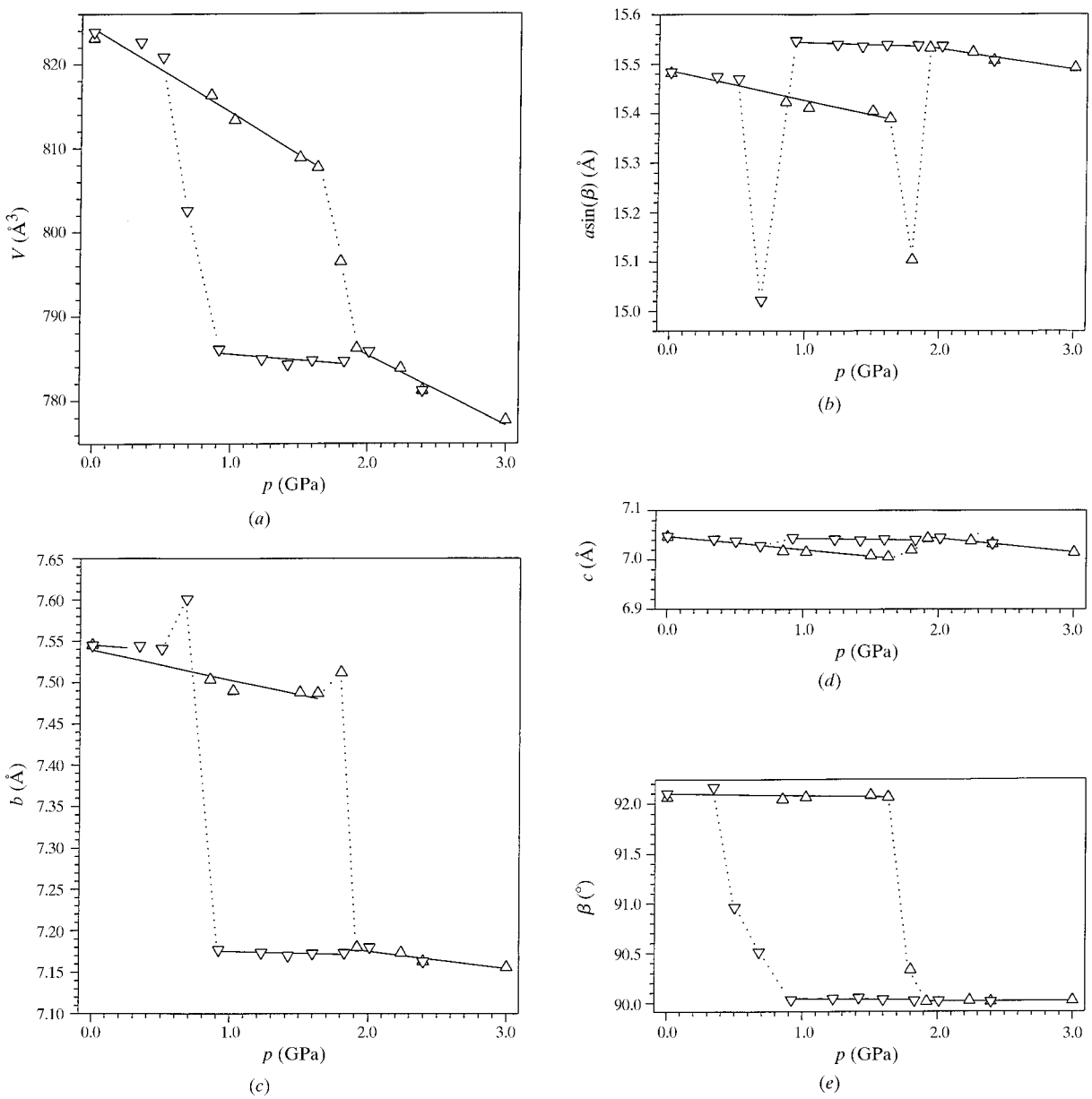

Fig. 2. Unit-cell parameters of NTP as a function of pressure. Δ denotes increasing pressure and ∇ denotes decreasing pressure. (*a*) Unit-cell volume *V versus* pressure; (*b*) unit-cell parameter *a versus* pressure; (*c*) unit-cell parameter *b versus* pressure [the scale of the ordinate is the same as part (*b*)]; (*d*) unit-cell parameter *c versus* pressure [the scale of the ordinate is the same as part (*b*)]; (*e*) monoclinic angle *β versus* pressure.

Bolotina, Simonov *et al.*, 1994). In the basis monoclinic (pseudo-orthorhombic) lattice with the parameters $a = 15.492\ (2), b = 7.545\ (1), c = 7.047\ (1)$ Å, $\beta = 92.06\ (2)^{\circ}$ superstructural (satellite) reflections correspond to diffraction vectors $\mathbf{H} = h\mathbf{a}^* + k\mathbf{b}^* + l\mathbf{c}^* + m\mathbf{q}$, $\mathbf{q} = 3\gamma\mathbf{a}^* + \gamma\mathbf{c}^*$, $\gamma = 0.2, m = \pm 1, 2$. Pseudo-orthorhombicity of the lattice creates the necessary geometric conditions for twinning of monoclinic NTP crystals. In this case, according to Friedel's theory (Friedel, 1926), any symmetry element of the orthorhombic lattice (2/*m* 2/*m* 2/*m*) which is absent in the diffraction class (2/*m*) of NTP crystals can be a twinning symmetry element. In our case the misorientation of monoclinic components of the twin makes an angle of 4.12° about the 2_y axis and the twinning index is $n = 1$.

In the NTP crystals studied the twin volume ratio was found by comparing similar reflections from different components. This ratio was estimated as 1:1 and it remained constant within the pressure range until the phase transition to the orthorhombic phase.

After the phase transition to the orthorhombic phase, satellite reflections with the wave vector $\mathbf{q} = 3\gamma\mathbf{a}^* + \gamma\mathbf{c}^*$, $\gamma = 0.2$ vanish but new satellites with the wave vector $\mathbf{q} = \mathbf{a}^* + 0.5\mathbf{c}^*$ appear. The occurrence of such a modulation vector is equal to the doubling of the parameter *b* of the basis cell. In order to determine the space-group symmetry of this phase we measured a small intensity array at 2.24 (5) GPa. At this stage, we found that the (3 + 1)-dimensional space group of NTP is $Bmcm(0,\beta,1)s00$, $\beta = 0.5$ [$a = 15.524\ (2)$, $b = 7.174\ (1)$, $c = 7.039\ (2)$ Å, $\mathbf{q} = \mathbf{a}^* + 0.5\mathbf{c}^*$]; the corresponding three-dimensional space group is *Ibam* [$a' = a = 15.524\ (2), b' = 2b = 14.078\ (2), c' = c = 7.039\ (2)$ Å]. A similar thermal phase transition in NTP is observed at 523 K.

At decreasing pressures, the reverse transformation to the monoclinic phase takes place at 0.6 ± 0.3 GPa within a pressure range of 0.45 ± 0.15 GPa. The unit-cell parameters were determined at two pressures within the pressure range of the transition. At 0.68 (5) GPa the monoclinic angle β is 90.51 (3)° and at 0.50 (5) GPa β is 90.96 (4)°. The changes of the unit-cell parameters *a*, *b* and *c* correspond to the changes observed during the transformation at increasing pressure. Since the volume stays constant below the phase boundary found at increasing pressure, the jump in volume associated with the reverse transformation is 3.9%.

It should be stressed once again that under high pressures, the orthorhombic phase of NTP exists within a narrow range of pressures from 1.8 to 3.0 GPa. Within the pressure range 2.5–3.0 GPa NTP crystals are completely destroyed. Thus, in NTP crystals under high pressures, in contrast to numerous thermal phase transitions, only one phase transition can be observed, from a monoclinic to an orthorhombic phase. This phase transition is the same as the thermal phase transition in NTP at 523 K (see Table 1).

Table 3. *Unit-cell parameters of NFP as a function of increasing and decreasing pressure*

Rules indicate phase transitions.

p (GPa)	*a* (Å)	*b* (Å)	*c* (Å)	*V* (Å^3)
Atmospheric	15.504 (1)	7.400 (1)	7.114 (1)	816.2 (1)
0.24 (5)	15.495 (4)	7.379 (2)	7.108 (2)	812.7 (3)
0.52 (5)	15.476 (4)	7.358 (2)	7.099 (2)	808.4 (3)
0.76 (5)	15.459 (3)	7.338 (2)	7.090 (2)	804.3 (2)
1.06 (5)	15.438 (4)	7.309 (1)	7.078 (1)	798.7 (3)
1.31 (5)	15.420 (2)	7.296 (1)	7.070 (2)	795.4 (1)
1.80 (5)	15.402 (6)	7.246 (2)	7.056 (2)	787.1 (4)
2.23 (5)	15.386 (6)	7.210 (3)	7.042 (2)	781.2 (4)
2.60 (5)	15.372 (8)	7.198 (3)	7.039 (2)	778.9 (4)
2.80 (5)	15.367 (4)	7.190 (2)	7.029 (1)	776.6 (4)
3.01 (5)	15.361 (7)	7.165 (2)	7.024 (1)	773.1 (3)
3.33 (5)	15.351 (6)	7.145 (2)	7.017 (2)	769.5 (3)
3.50 (5)	15.340 (4)	7.110 (2)	7.009 (2)	764.5 (3)
4.02 (5)	15.331 (6)	7.100 (2)	7.001 (2)	762.1 (3)
4.20 (5)	15.329 (8)	7.088 (2)	6.998 (2)	760.4 (5)
5.00 (5)	15.309 (4)	7.020 (2)	6.967 (2)	748.7 (3)
5.59 (5)	15.297 (6)	7.024 (1)	6.925 (1)	744.1 (3)
5.82 (5)	15.307 (5)	7.020 (2)	6.906 (2)	742.1 (3)
6.21 (5)	15.382 (4)	6.998 (2)	6.853 (2)	737.7 (3)
7.00 (5)	15.376 (4)	6.956 (2)	6.813 (2)	728.7 (3)
7.99 (5)	15.362 (6)	6.926 (2)	6.789 (3)	722.3 (4)
9.65 (5)	15.326 (5)	6.860 (2)	6.734 (2)	708.0 (3)
11.02 (5)	15.301 (8)	6.842 (2)	6.690 (3)	700.4 (5)
12.00 (5)	15.275 (6)	6.832 (2)	6.679 (2)	697.0 (2)
12.00 (5)	15.275 (6)	6.832 (2)	6.679 (2)	697.0 (2)
10.70 (5)	15.309 (2)	6.841 (1)	6.689 (1)	700.4 (1)
10.00 (5)	15.323 (3)	6.857 (1)	6.720 (1)	706.5 (1)
9.70 (5)	15.326 (4)	6.861 (1)	6.734 (2)	708.4 (2)
9.20 (5)	15.343 (3)	6.879 (1)	6.741 (1)	712.1 (2)
8.00 (5)	15.365 (4)	6.920 (1)	6.777 (2)	720.2 (3)
7.60 (5)	15.371 (6)	6.945 (2)	6.792 (1)	722.5 (4)
6.30 (5)	15.386 (5)	6.990 (1)	6.842 (1)	735.8 (2)
5.40 (5)	15.391 (4)	7.048 (2)	6.863 (2)	744.5 (4)
4.83 (5)	15.411 (2)	7.123 (2)	6.898 (2)	757.2 (2)
3.60 (5)	15.351 (4)	7.131 (2)	7.018 (3)	766.2 (4)
3.25 (5)	15.358 (6)	7.135 (1)	7.022 (1)	769.1 (3)
2.90 (5)	15.367 (6)	7.161 (3)	7.032 (1)	773.1 (5)
2.60 (5)	15.375 (8)	7.187 (2)	7.042 (1)	781.3 (4)
2.30 (5)	15.388 (5)	7.210 (2)	7.044 (1)	781.6 (3)
1.82 (5)	15.398 (4)	7.235 (2)	7.051 (1)	785.5 (3)
1.48 (5)	15.407 (8)	7.260 (2)	7.059 (1)	789.6 (5)
1.01 (5)	15.430 (5)	7.311 (1)	7.077 (1)	798.4 (3)
Atmospheric	15.504 (1)	7.401 (1)	7.114 (1)	816.2 (1)

5.2. *NFP crystals*

Refined lattice parameters of the orthorhombic basis lattice of NFP under pressures from atmospheric to 12.0 GPa are listed in Table 3. Corresponding plots as a function of pressure are shown in Figs. 3(*a*)–3(*d*).

The changes that occur in NFP crystals bring about changes in the color of the samples. First, the color changes from dark orange (red) to pink starting at ~1.5 GPa and up to ~2.0 GPa, then the color changes from pink to violet at 6.0 GPa.

Taking into account all the information contained in Fig. 3, a third phase transition is indicated. The first phase transition is best seen from a sudden change in the slope of the pressure dependence of the unit-cell parameter a at 1.39 ± 0.08 GPa (Fig. 3*b*) and the second in a change of the slope of c at 4.52 ± 0.32 GPa (Fig. 3*d*). The unit-cell parameter b of the second high-pressure phase increases if the pressure is increased. The third phase transition is most clearly indicated by a jump of the unit-cell parameter a, which increases suddenly at 6.02 ± 0.20 GPa (Fig. 3*b*).

As there are no distinct discontinuities in the volume associated with these phase transitions, a common Birch–Murnaghan equation of state was fitted to the data. The bulk modulus and the pressure derivative were $K_0 = 46$ (1) GPa and $K_0' = 5.7$ (4).

Owing to a large hysteresis (ΔP_i) associated with the third phase transition, the second high-pressure phase

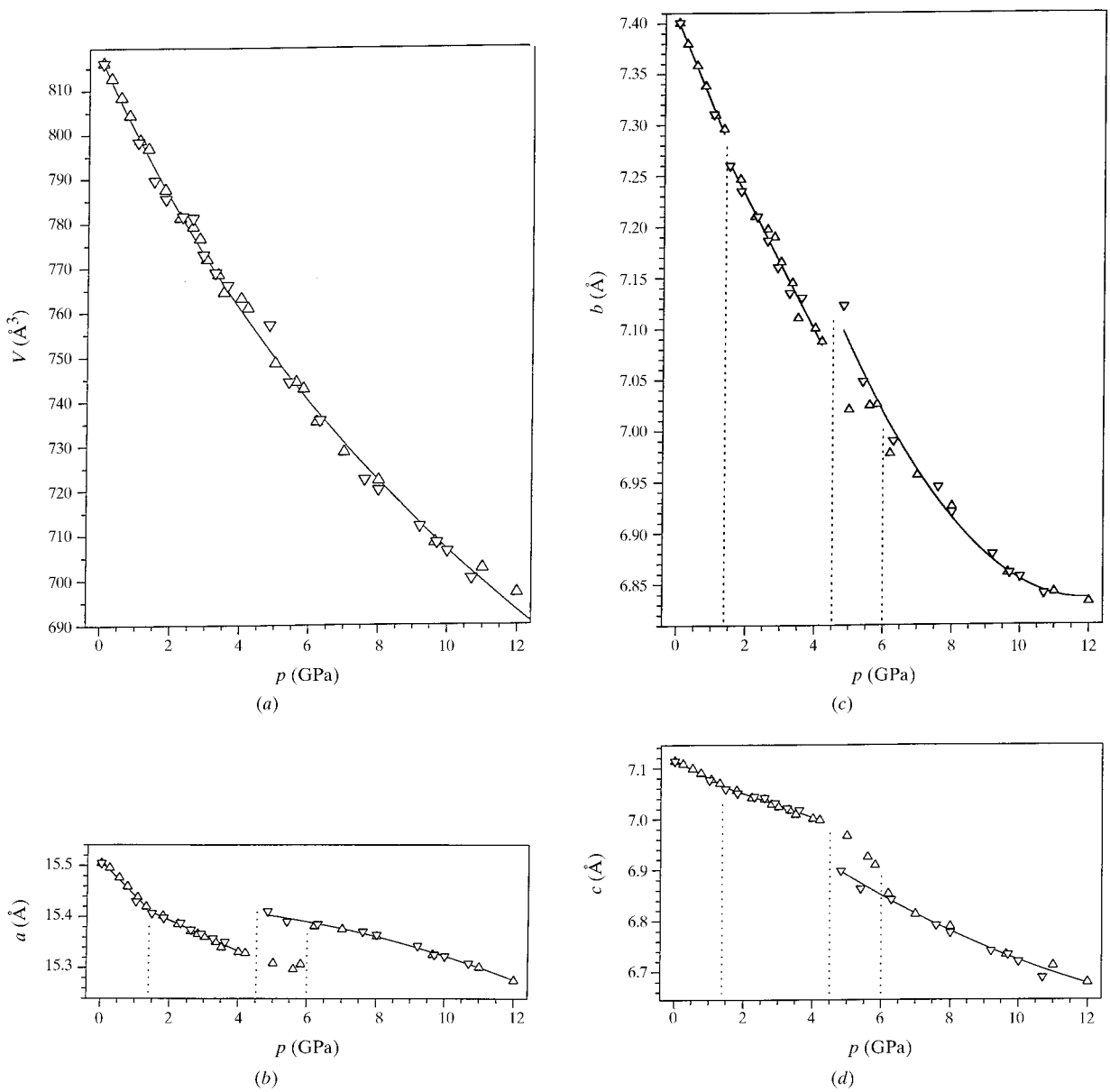

Fig. 3. Unit-cell parameters of NFP as a function of pressure. ∇ denotes increasing pressure and Δ denotes decreasing pressure. (*a*) Unit-cell volume V *versus* pressure (the line drawn represents a fit to a Birch–Murnaghan equation of state); (*b*) unit-cell parameter a *versus* pressure; (*c*) unit-cell parameter b *versus* pressure [the scale of the ordinate is the same as part (*b*)]; (*d*) unit-cell parameter c *versus* pressure [the scale of the ordinate is the same as part (*b*)].

can not be observed if the pressure is decreased from above 6.0 GPa. The third high-pressure phase transforms back directly to the first high-pressure phase at 4.2 ± 0.6 GPa, as is obvious from the pressure dependence of the unit-cell parameters a and b (Figs. 3*b* and 3*c*, respectively).

In order to elucidate the space-symmetry changes which occur at these phase transitions, we measured two intensity arrays, at 4.00 (5) GPa (pink sample) and 10.00 (5) GPa (violet sample). Analysis of X-ray measurements showed that on changing from atmospheric pressure [$a = 15.504$ (1), $b = 7.401$ (1), $c = 7.114$ (1) Å] to 4.0 GPa [$a = 15.331$ (6), $b = 7.101$ (1), $c = 7.001$ (1) Å] (3 + 1)-dimensional space symmetry is retained in NFP crystals: $Bmcm(0,\beta,1)s00$, $\beta = 0.5$ [the appropriate three-dimensional space group is *Ibam* ($a' = a$, $b' = 2b$, $c' = c$)]. At 10.0 GPa, *i.e.* above the pressure of the last phase transition observed, superstructure reflections on the half-period **b*** vanish. Therefore, like the thermal phase transition at 530 K (Table 1), one might suppose that in NFP above 6.0 GPa an incommensurately modulated phase with an irrational component γ**c*** of the wave vector is formed. Unfortunately, in our experiments no satellite reflections on distances vector $\pm\gamma$**c*** from the points of the basis reciprocal lattice were detected. In view of the expected weak intensity of the satellite reflections, more reliable information can be obtained by using more powerful (*e.g.* synchrotron) radiation.

This work has been financially supported by the Alexander von Humboldt Foundation and in part by the Russian Fundamental Investigations Foundation (grant No. 97-05-64647).

References

Bolotina, N. B., Maximov, B. A.,Tamazyan, R. A. & Klokova, N. E. (1993). *Crystallogr. Rep.* **38**, 451–454.

Friedel, G. (1926). *Lecons de Cristallographie*. Reprinted 1964. Paris: A. Blanchard.

Ivanov-Schitz, A. K. & Sigaryev, S. E. (1990). *Solid State Ion.* **40/41**, 76–78.

Klokova, N. E., Maximov, B. A. & Tamazyan, R. A. (1993). *Crystallogr. Rep.* **38**, 454–456.

Maximov, B. A., Bolotina, N. B., Simonov, V. I., Petříček, V. & Schulz, H. (1994). *Acta Cryst.* B**50**, 261–268.

Maximov, B. A., Bolotina, N. B., Tamazyan, R. A. & Schulz, H. (1994). *Z. Kristallogr.* **209**, 649–656.

Maximov, B. A., Klokova, N. E., Verin, I. A. & Timofeeva, V. A. (1990). *Sov. Phys. Crystallogr.* **35**, 497–500.

Merill, L. & Bassett, W. A. (1974). *Rev. Sci. Instrum.* **45**, 290–294.

Tamazyan, R. A., Maximov, B. A., Bolotina, N. B., Novikova, N. E. & Simonov, V. I. (1994). *Crystallogr. Rep.* **39**, 422–427.